Electronic Supplementary Material (ESI) for Soft Matter.

Supplementary Information for

Bijels stabilized using rod-like particles

Niek Hijnen,[a] Dongyu Cai[a] and Paul S. Clegg[a*]

School of Physics and Astronomy, University of Edinburgh, Peter Guthrie Tait Road, Edinburgh, EH9 3FD, UK

1. Experimental methods

1.1 Materials

Ethylene glycol (anhydrous, 99.8%), hexamethyldisilazane (HMDS, reagent grade, ≥99%), Nile Red (technical grade) and fluorescein were used as received from Sigma Aldrich. Rhodamine B (99+%) and nitromethane (99+%, stored under nitrogen) were obtained from Acros Organics. Ethanol (absolute) was obtained from VWR, and ammonium hydroxide solution (35%, reagent grade) was obtained from Fisher Scientific.

1.2 Tuning surface chemistry of colloids

For each batch of particles (after synthesis only washed with ethanol) a stock dispersion of known concentration (by weight) in ethanol was prepared. HMDS treatment of colloids to modify their wetting properties was done iteratively to find conditions resulting in bijel formation, as described below. This was performed on small samples (in 7 mL vials), by diluting down the stock suspension with ethanol to obtain a suspension of approximately 0.3 g rods (0.1 g spheres) in 4 g ethanol. Then, HMDS was added (typically ~0.1 g for rod-bijels, and ~0.07 g for sphere-stabilized bijels) followed by 0.3-0.4 g ammonium hydroxide solution (35%). The obtained mixture was stirred for 24 hours (6 pit, 1000 rpm). Subsequently, particles were washed 5 times in the same vial with ethanol, and finally dried. For drying (~100 °C, Binder VD23 oven set to 121 °C) first bulk solvent was allowed to evaporate in 30 minutes, after which the solid layer of particles was ground into a more fine powder using a spatula (this appears to be important to get the wetting right). Finally, drying was continued for another 60 minutes, but now under full vacuum. Particles were mostly used immediately after drying, but when they needed to be stored they were kept in tightly sealed vials within a desiccator.

1.3 Sample preparation and imaging

For all samples, including throughout the iterative process working towards bijel-forming particles, the same procedure was followed. Dry particles were directly dispersed in a nitromethane (NM)/ethylene glycol (EG) mix (64 wt% nitromethane) using a hot ultrasonic bath (1.7 mL vials, 50 °C, 15 minutes). Vials containing the samples were then transferred into an aluminium mantle heated (50 °C) using a hotplate. Quickly, VitroCom capillaries, heated on the same hotplate, were filled by dipping them into the hot sample, and then quenched onto an aluminium block (23 °C). Samples were then fixed on a glass slide using silicone sealant on both ends. Finally, they were studied using a Zeiss LSM 700 confocal with an oil immersion objective (40× or 63×), and in some cases also a 20× objective was used. For imaging with the 20× and the 40× oil-immersion objective 0.2×4 mm capillaries were used, and for the 63× oil-immersion objective 0.1×2 mm capillaries were used. FITC (rods) and fluorescein (EG) were excited with a 488 nm laser line, and Nile Red (NM) and RITC (spheres) were excited with a 555 nm laser line. Emitted fluorescence of the 2 dyes present in a sample was sent to separate photomultipliers, split at 530 nm using a variable dichroic mirror. The light going to the PMT receiving > 530 nm (from Nile Red or RITC) was passed through a 560 nm long-pass filter.

2. The formation of rod-stabilized emulsions

The wettability (or contact angle) is dependent on HMDS concentration with the remaining reacting parameters fixed. Since the phase diagram in Figure 1a, as shown in the main text, is symmetric, this leads to approximately equal volumes of NM-rich and EG-rich phase when the single fluid with the rods follows the quenching pathway (indicated by the arrow) for spinodal decomposition. With the NM-rich phase and rods labelled by Nile Red and FITC, respectively, bijel formation is attempted with every batch of modified rods to follow the change in wettability. Figure S1a shows that the NM-rich droplets are stabilized by the rods modified at low HMDS concentration. Figure S1b demonstrates that the inversion of the emulsion occurs when the HMDS concentration is significantly increased. This transition is helpful for us to narrow down the range for searching the appropriate amount of HDMS required by neutral wet rods.

The rods trapped on the droplets have silica shells that are composed of a thin inner layer labelled with a fluorescent dye, and a thick unlabelled outer layer, allowing their packing to be resolved. Closer to neutral wetting of the particles, more oddly shaped droplets are formed, and at higher magnification details start to be revealed in Figure S2a. In general it can be seen that the stabilizing layer of rods are quite rough. While less obvious for larger droplets, small droplets have clearly angular shapes, with facets on the scale of the rod-length. Zooming in on the droplets, the arrangement of the particles can be observed in some detail (Figure S2b). Some local ordering is observed in the form of small side-side stacks of rods. The roughness of the stabilizing layer appears to originate from rods sticking out and overlapping each other.

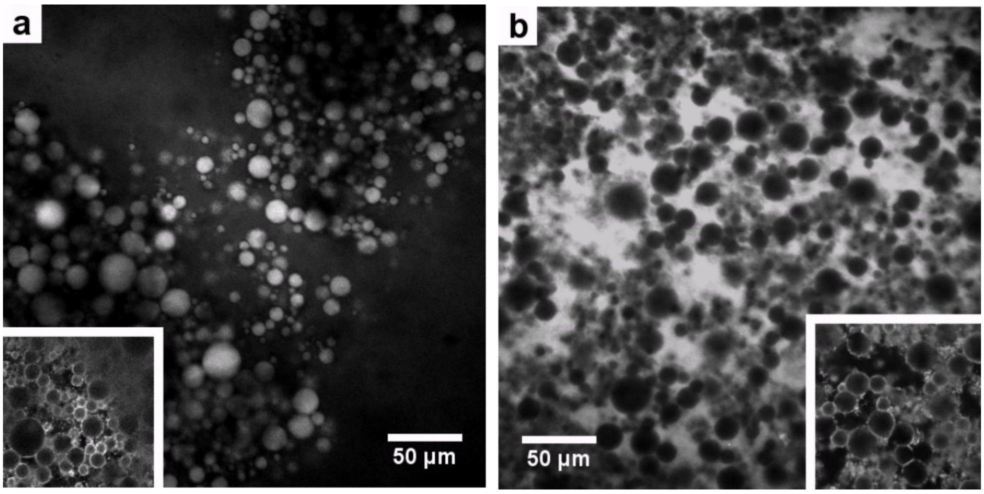

Fig. S1 Pickering emulsions resulting from a temperature quench in the presence of rods modified with HMDS at a (a) low, and (b) high concentration. The main images show Nile Red fluorescence from the NM-rich phase, and insets show FITC fluorescence from the rods.

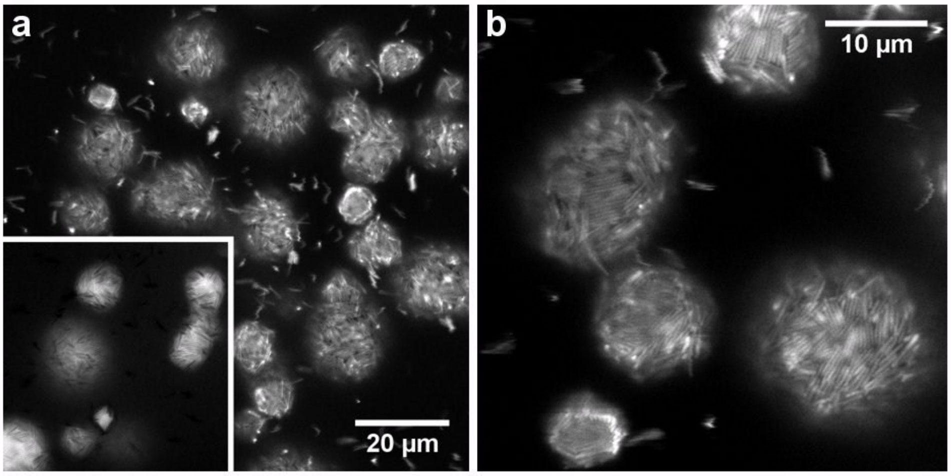

Fig. S2 High magnification images (63×objective) of rod-stabilized droplets resulting from a spinodal decomposition of the host solvent. (a) An image showing the FITC fluorescence from the rods for a larger collection of droplets at lower magnification, with the inset showing Nile Red fluorescence from the NM-rich phase. (b) A higher magnification image showing the FITC fluorescence from the rods, giving a closer look at the structuring of the particles.

3. Quantification of the domain size of the bijels.

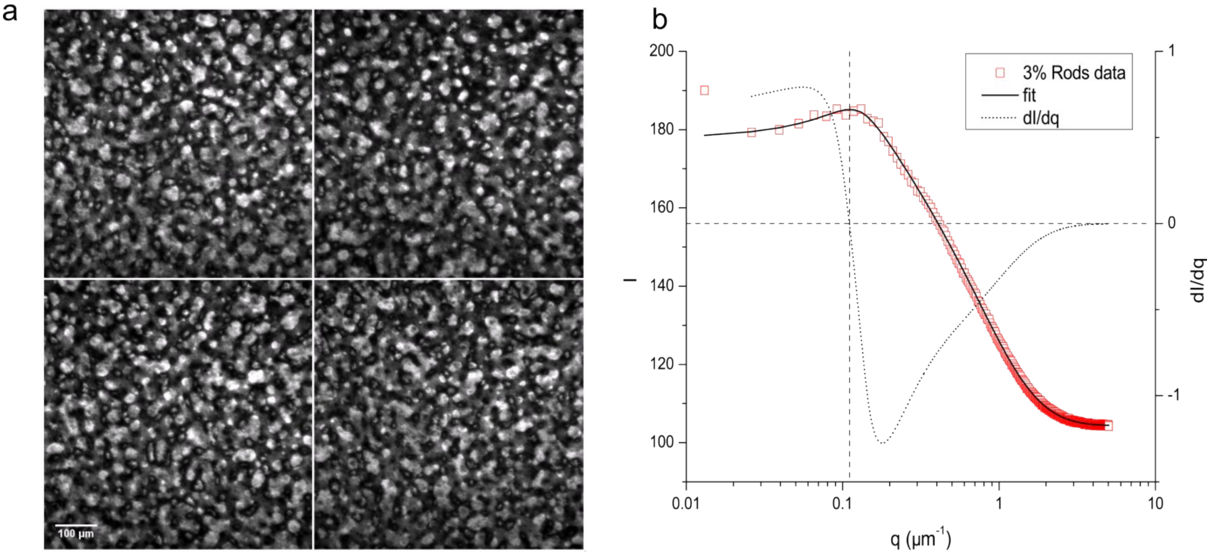

Fig. S3 (a) Some more examples of images (3vol.% rods) used to obtain the domain size as described in the main text. (b) An example demonstrating how q_{knee} was obtained from an average of the radially averaged FFTs of several images like those in Panel (a) (red, empty squares). A fit (solid black line) overlaps the data, and a dotted black line plots the local slope (dI/dq) of the curve.

To quantify the domain size of each bijel sample, several images like those shown in Figure S3a were used. The images were obtained at different locations in the sample (see Figure S3a for a few examples from the same sample). By taking the radial averages of their squared 2D Fourier transforms, the structure factors were calculated. Those belonging to a single set of a particular sample were averaged (for example, the red squares in Figure S3b) to improve statistics. The dominant length scale in the sample, the domain size, is represented by a knee in the curve at the corresponding wave vector (q). This is similar to observations in SANS measurements of sponge phases in surfactant solutions,[1,2] the structure of which is a (dynamic) analogue to the bijel structure.

To extract q corresponding to the knee, the curves were fitted to a function comprised of the shifted average of 2 slightly adapted cumulative distribution functions. The model has 9 fitting parameters and consequently can give a very good correspondence to the data. Fitting yields a smooth curve with a well-defined knee, the peak of which was located by numerical differentiation (Figure S3b).

4. Packing fraction for sphero-cylinders

To complete our analysis we need to know how the expected packing fraction of sphero-cylinders depends on their aspect ratio, A. Objects of this shape cannot reach a packing fraction of 1 due to the spherical end caps. These end caps are best packed when they are inter-leaved (like close-packed disks). Three sphero-cylinders, of length L and radius r, meeting are sketched below:

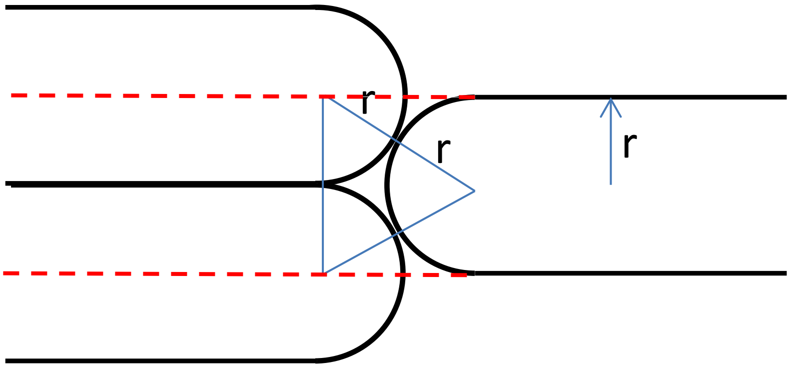

The aspect ratio is then: $A = {}^{L}/_{2r}$

The length of the straight section of the sphero-cylinders is: $d = L - 2r$

The red dashed lines delineate the motif which is repeated throughout the packing. A section of this width ($2r$) includes two complete interstitial spaces. We make this unit cell length $d + h$ where $h = \sqrt{3}r$ the height of the blue triangle. This unit cell extends from the centre of the sphero-cylinders on one side of the junction to the centre of the sphero-cylinder on the other side of the junction.

Area of surface where sphero-cylinders are situated $= (d + \sqrt{3}r)\ 2r$

Area of occupied by sphero-cylinders $= 2dr + (2r\ h)\ {}^{\pi}/_{2\sqrt{3}} = 2dr + \pi r^2$

Thus the packing fraction is

$$\nu = \frac{d + {}^{1}/_{2}\pi r}{d + \sqrt{3}r}$$

$$\nu = \frac{L - r\left(2 - {}^{\pi}/_{2}\right)}{L - r(2 - \sqrt{3})}$$

$$\nu = \frac{1 - (1 - \pi/4)/A}{1 - (1 - \sqrt{3}/2)/A}$$

where A is the aspect ratio.

5. Formation of ‘monogels’

It was previously found in water/2,6-lutidine bijels that the particle structure can remain intact after re-mixing of the liquids [3]. The resulting material was termed ‘monogel’. Successful monogel formation in NM/EG was here observed upon prolonged aging of samples. For a sample aged 13 days, heating a sample to 50 °C resulted in a collapse of the structure, leaving bigger aggregates of particles (Figure S4a). The Nile Red fluorescence drops significantly as mixing occurs, related to the changed solvent composition and the presence of large aggregates. Increasing aging time to 19 days, the particle structure remains intact when the liquid phases re-mix after heating the sample to 50 °C, so a monogel is formed (Figure S4b). In contrast, in water/2,6-lutidine only 20 minutes of aging is required for monogel formation [4]. Here, mixing of the liquid phases is observed by Nile Red fluorescence, which decreases as the solvent composition changes, while contrast differences disappear, except for the black ‘imprint’ caused by the particle structure.

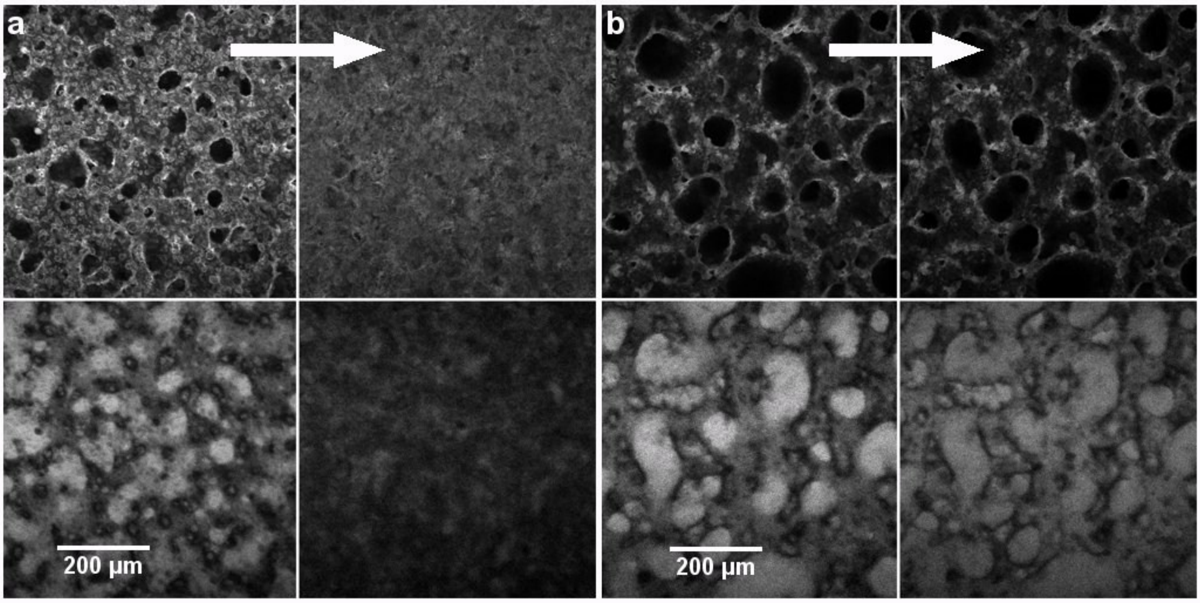

Figure S4 Monogel formation in NM/EG. (a) Structure aged for 13 days, heated to 50 °C. (b) structure aged for 19 days, heated to 50 °C.

References
1 D. Gazeau and A. M. Bellocq, *Europhys. Lett.*, 1989, **9**, 447.
2 D. Roux, C. Coulon and M. E. Cates, *J. Phys. Chem.*, 1992, **4187**, 4174.
3 E. Sanz, K. A. White, P. S. Clegg and M. E. Cates, *Phys. Rev. Lett.*, 2009, **103**, 255502.
4 M. N. Lee, J. H. J. Thijssen, J. A. Witt, P. S. Clegg and A. Mohraz, *Adv. Funct.Mater.*, 2013, **23**, 417.